Optical Engineering

SPIEDigitalLibrary.org/oe

Polymeric nanolayered gradient refractive index lenses: technology review and introduction of spherical gradient refractive index ball lenses

Shanzuo Ji
Kezhen Yin
Matthew Mackey
Aaron Brister
Michael Ponting
Eric Baer

SPIE

Polymeric nanolayered gradient refractive index lenses: technology review and introduction of spherical gradient refractive index ball lenses

Shanzuo Ji
Kezhen Yin
Matthew Mackey
Aaron Brister
Case Western Reserve University
Center for Layered Polymeric Systems
Department of Macromolecular Science and Engineering
2100 Adelbert Road, Cleveland, Ohio 44106

Michael Ponting
PolymerPlus LLC
7650 Hub Parkway
Valley View, Ohio 44125
E-mail: mponting@polymerplus.net

Eric Baer
Case Western Reserve University
Center for Layered Polymeric Systems
Department of Macromolecular Science and Engineering
2100 Adelbert Road, Cleveland, Ohio 44106

Abstract. A nanolayered polymer films approach to designing and fabricating gradient refractive index (GRIN) lenses with designer refractive index distribution profiles and an independently prescribed lens surface geometry have been demonstrated to produce a new class of optics. This approach utilized nanolayered polymer materials, constructed with polymethylmethacrylate and a styrene-co-acrylonitrile copolymer with a tailorable refractive index intermediate to bulk materials, to fabricate discrete GRIN profile materials. A process to fabricate nanolayered polymer GRIN optics from these materials through thermoforming and finishing steps is reviewed. A collection of technology-demonstrating previously reported nanolayered GRIN case studies is presented that include: (1) the optical performance of a f/# 2.25 spherical GRIN plano-convex singlet with one quarter (2) the weight of a similar BK7 lens and a bio-inspired aspheric human eye GRIN lens. Original research on the fabrication and characterization of a Luneburg inspired GRIN ball lens is presented as a developing application of the nanolayered polymer technology. [DOI: 10.1117/1.OE.52.11.112105]

Subject terms: gradient refractive index; polymer; lenses; imaging; solar refractive index; nanolayers.

Paper 130379SS received Mar. 8, 2013; revised manuscript received Jun. 10, 2013; accepted for publication Jun. 11, 2013; published online Jul. 25, 2013.

1 Introduction

Optimized for survival, biological species evolved internal gradient refractive index (GRIN) lenses for maximizing their visual performance. Homogeneous lenses, which are constructed from a uniform refractive index material, alter light's direction only at its surfaces as a function of the optic's geometry and incident and emergent light angles. On the other hand, GRIN lenses are constructed from materials whose refractive indices are continually changing which refract the propagating light through the bulk material as well as that of the optic surface. Therefore, the optical power of GRIN lenses is not only determined by its surface geometry, but also by the spatial distribution of refractive index occurring through the thickness of the optic. As an example, a GRIN optic with spherical refractive index profile that is decreasing in magnitude from a center maximum to a surface minimum refractive index can centrally slow the propagating light so that peripheral light rays can intersect it at the same point along the lens' optical axis.[1] Combining this effect with the traditional tool of geometric power derived from a surface curvature equips GRIN containing visual systems with enhanced focusing power and an increased view field while minimizing optical aberrations, lens size, and complexity.[1–3]

Animals with simple camera-type eyes focus an image onto a single retinal photoreceptor. Aquatic creatures, such as the fish,[4] octopus,[5] squid,[6] and jellyfish[7] have camera-type eyes which contain GRIN lenses to compensate for low contrast between water ($n = 1.33$) and protein refractive indices.[8] Since biological lens protein refractive indices range between 1.33 and 1.52, values similar to water, aquatic eyes need to exploit strongly curved surface geometries and GRIN to derive stronger optical power. Without GRIN optics, spherically curved homogenous lenses could still focus light and offer large fields of view, however, they would exhibit significant spherical aberrations and focused light would not intersect at one point along the lens's optical axis, causing image blur.[1–3] By contrast, air-dwelling creatures,[9–12] such as the lion, cow, rat, and human, utilize GRIN lenses to correct for significantly larger geometric aberrations stemming from a larger difference in environment (air $n = 1.0$) to lens material ($n = 1.33$ to 1.43) refractive index as well as contributions from aspheric-shaped lenses (Table 1). A bi-product of nature's incorporation of GRIN into eye lens optics has resulted in most biological imaging systems containing a low, typically one to three, number of lenses, which minimizes the size necessary for an organism's eyes to exhibit a powerful accommodating image system.

In contrast to nature, state-of-the-art synthetic optical designs typically utilize a series of homogenous refractive index elements to form images. Aberrations are corrected by including aspheric optical surface geometries and combining materials with varying degrees of dispersion in the system design. Typically consisting of glass or plastic lenses, it is not uncommon for high definition optical zoom systems to consist of five or more elements. This traditional multi-material, multi-element design approach has been successfully applied by optical engineers for decades. However, these result in systems with larger element counts, larger size, and higher weight than naturally occurring GRIN analogs.[13]

Table 1 Properties of GRIN lenses is aquatic creatures and air-dwelling animals.

Environment	Animal	Δn	GRIN distribution	Lens geometry
Aquatic	Trout[4]	0.22	Parabolic	Spherical
	Octopus[5]	0.15	Parabolic	Spherical
	Squid[6]	0.21	Parabolic	Spherical
	Jellyfish[7]	0.14	Parabolic	Spherical
Air	Rat[9,10]	0.11	Parabolic	Aspheric
	Cow[9,10]	0.08	Parabolic	Aspheric
	Lion[9,10]	0.04	Modified parabola	Aspheric
	Human[11,12]	0.05	Modified parabola	Aspheric

The technological limitations of successfully demonstrated GRIN lens fabrication techniques, such as ion exchange,[14] partial polymerization,[15] interface-gel copolymerization,[16] chemical vapor deposition,[17] and plasmonics[18] have minimized their application. Specifically, these lenses are limited by their refractive index distribution magnitudes (Δn), refractive index profiles (linear, Gaussian, and Lorentzian), and their small apertures.[19] While these technologies have their limitations, another approach discovered in 2004 by Case Western Reserve University and the Naval Research Laboratory produces GRIN lenses through nanolayering of polymeric films.[20] This unique materials approach has enabled the fabrication of GRIN lenses with an unprecedented variety of GRIN profiles, index distribution magnitudes, geometries, and lens apertures.[21–26] This paper reviews the enabling technology and describes unique nanolayered polymeric GRIN lenses, including original research demonstrating the fabrication of a polymeric-layered GRIN ball lens. These GRIN lenses demonstrate the technology's potential to utilize unrestricted lens geometries and refractive index profiles to improve lens performance, realize optical element savings, and reduce optical system size and weight.

2 GRIN Optic Fabrication Technique Based on Nanolayered Polymeric Films

2.1 *Enabling Technology: Polymer Films with Layer Thickness <λ/4*

The technological basis for creating nanolayered polymer GRIN optics lies in the fabrication of polymer films with a tailored refractive index (Fig. 1). When two polymer materials with a sufficient difference in refractive index are arranged in alternating layers, the resulting layered material has a refractive index modulation whose period corresponds to layer thicknesses.[21] These layered polymer materials have interesting optical properties when individual layer thicknesses are similar to or shorter than a wavelength of light. In the first case, where the wavelength of light is one quarter ($\lambda/4$) of the film's repeating layer thicknesses, the material exhibits optical reflectivity. This high reflectivity makes it a one-dimensional (1-D) photonic crystal.[27,28] In the second case, when the layer thickness is less than one quarter of the wavelength of light, the layered polymeric material transmits light.[23] These multilayered films with individual layer thicknesses less than the quarter wavelength of light also exhibit an overall bulk film refractive index that is the volumetric average of the two component materials (Fig. 2). It is under this second condition, where the layered materials have individual layer thicknesses less than $\lambda/4$, that nanolayering polymeric materials enable a unique, polymer film coextrusion-based approach to GRIN lens fabrication.

2.2 *Enabling Technology: Forced Assembly Multilayer Coextrusion*

The initial step in fabricating GRIN optics is the production of a polymer films series via forced assembly multilayer coextrusion processing. Multilayer coextrusion is a continuous processing technique creating films composed of tens to thousands of micrometer or nanometer thick layers. Utilizing a two-component coextrusion system, two single screw extruders with melt metering pumps supply two polymers, "A" and "B", into a layered feedblock. The metering pumps add a degree of volumetric control over the relative materials, which enables variation in the nanolayered film's volumetric composition, therefore also defining the material's bulk refractive index. Using this system, polymers A and B are layered so polymer B is sandwiched between two A layers in an A/B/A construction internal to a three-layer coextrusion feedblock. Starting from this feedblock, the A/B/A polymer layers flow into a series of layer multiplying die elements. Each layer multiplier die doubles the initial feed stream's layer count through a process of flow splitting, compression, and vertical stacking, as shown in Fig. 1(a) and described in Ponting et al.[29] Thus, one A/B/A layered stack is placed on another creating an A/B/A/B/A layered stack. When combined in series, n number of multiplier elements produces multilayered films consisting of $2^{(n+1)}+1$ alternating layers. Figure 1(a) represents a two-component coextrusion system and a series of 11 multiplier elements that increase the number of layers from 3 to 4097. This coextrusion process produced 4097 nanolayered polymer films with overall bulk film thickness of 50 μm. The 50 μm target was selected to ensure that each of the 4097 intra-film layers was significantly below the $\lambda/4$ limitation. This criterion satisfies the physical requirement for the volumetric additive refractive index rule of mixtures applied to nanolayered films.

2.3 *Tailored Refractive Index Nanolayered Polymer Films*

Polymer films of 4097 poly(methyl methacrylate) (PMMA, Arkema Plexiglas V920) and poly(styrene-co-acrylonitrile) with 17 mol% acrylonitrile (SAN17, Ineos Lustran Sparkle) layers were coextruded for constructing GRIN optics. The volumetric contribution of PMMA to SAN17 was varied in 2% steps, so their respective contributions were 100/0, 98/2, 96/4, continuing through 50/50, and ending at 0/100, respectively. Together, this series produced 51 separate films of PMMA/SAN17, volumetrically varied in 2% steps, each engineered so that their total film thickness was 50 μm. As an example, a 50/50 volumetric ratio of PMMA/SAN17

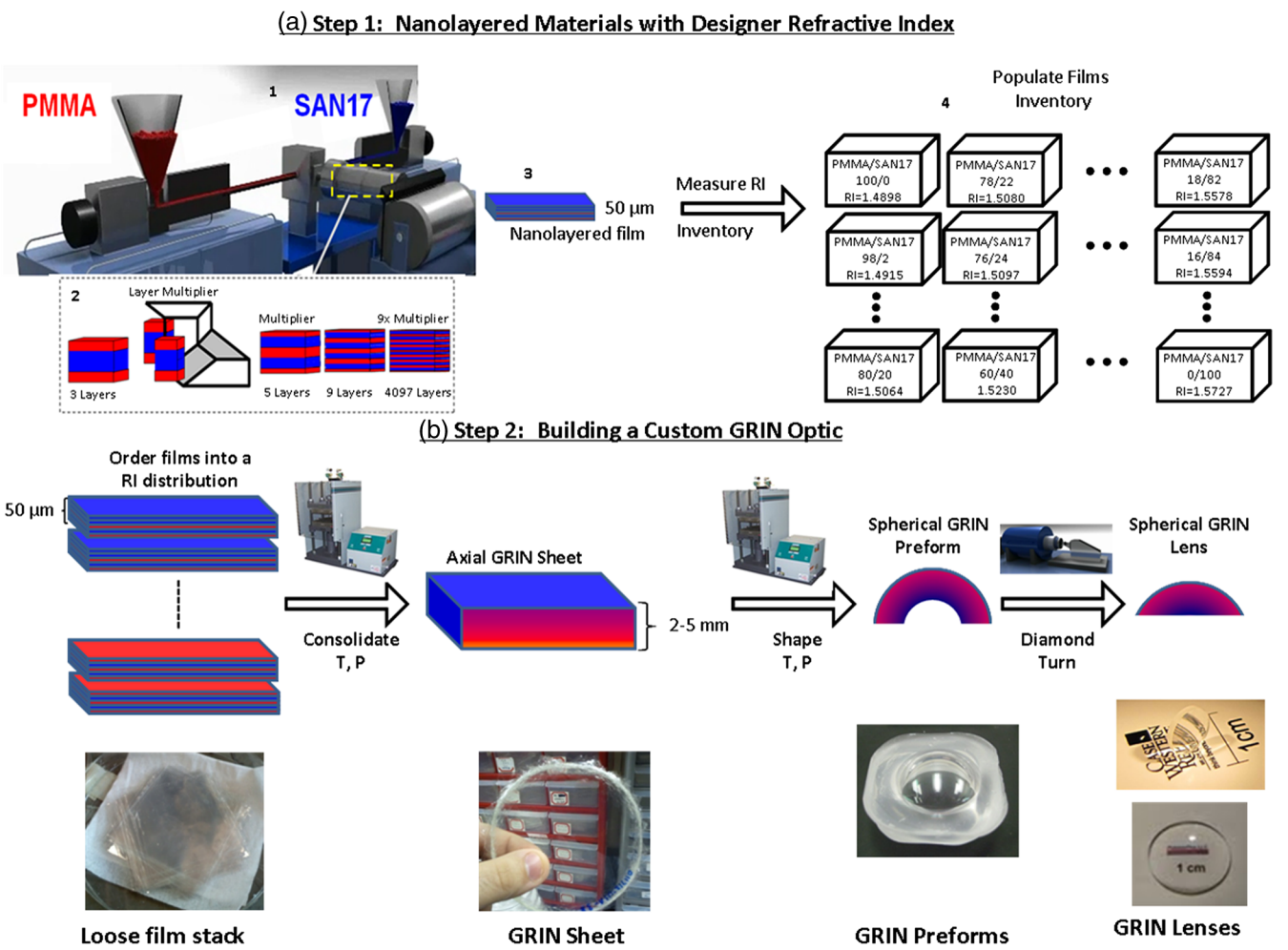

Fig. 1 (a) Layout of two component forced assembly multilayer system: extruders, polymer melt pumps, feedblock, multilayering dies, surface layer extruder (not shown), and exit die. Layer multiplication from two to four layers is illustrated by cutting, squeezing, spreading, and recombining polymer melt streams; and (b) procedure to build a GRIN lens: stacking, consolidation, shaping, and diamond turning.

nanolayered film with an overall thickness 50 μm will have about a 12-nm individual intra-film layer thickness (50 μm divided by 4097 layers) because each polymer is volumetrically proportional. The refractive indices of these 51 layered films processed at 2% compositional step intervals were measured via a Metricon refractometer and exhibited a 0.0016 difference in their bulk film refractive index, which was predicted [Fig. 2(a)].[21,22] These results are plotted as a function of overall PMMA film volume percentage in Fig. 2(b). Theoretically, it is possible to make polymer films of any refractive index value between its constituent polymers, such as PMMA or SAN17. These 51 compositional films were selected based on computational simulations suggesting the 0.0016 refractive index step size in the GRIN lens was sufficient to demonstrate a satisfactory optical performance. Next, these 51 nanolayered films were utilized to construct a GRIN polymer media.

2.4 *Construction of a Gradient Refractive Index Profile*

A fundamental strength of the polymeric nanolayered approach is the removal of refractive index profile shape restrictions since any value intermediate to the constituent polymer absolute refractive index values can be used. Thus, constructing a refractive index gradient is accomplished by sequentially stacking nanolayered PMMA/SAN17 polymer films whose refractive indices vary [Fig. 1(b)]. The nanolayered polymer film stacks can be arranged so their refractive index profiles are linear, a second-order polynomial shape, a third-order polynomial shape, and so on, as shown in Fig. 3. Typically, stacks consist of between 75 and 300 individual nanolayered films. Once the desired refractive index distribution profile is stacked, typically in a clean room environment to prevent contamination, a thermoforming consolidation process is completed at elevated temperatures and pressures to lock-in the desired axial GRIN profile. This consolidated GRIN stack is usually a 3- to 7-mm thick flat sheet that possesses an axial refractive index distribution normal to the surface plane.

2.5 *GRIN Optics Finishing*

Subsequent shaping, polishing, or diamond turning steps to the consolidated axial GRIN sheet enable the construction of axial, spherical, or radial GRIN optics. Converting an axial GRIN sheet to a radial or spherical GRIN distribution is accomplished by a second thermoforming operation. Within this operation, an axial GRIN sheet is formed into a meniscus-like lens, or GRIN preform. This is done by

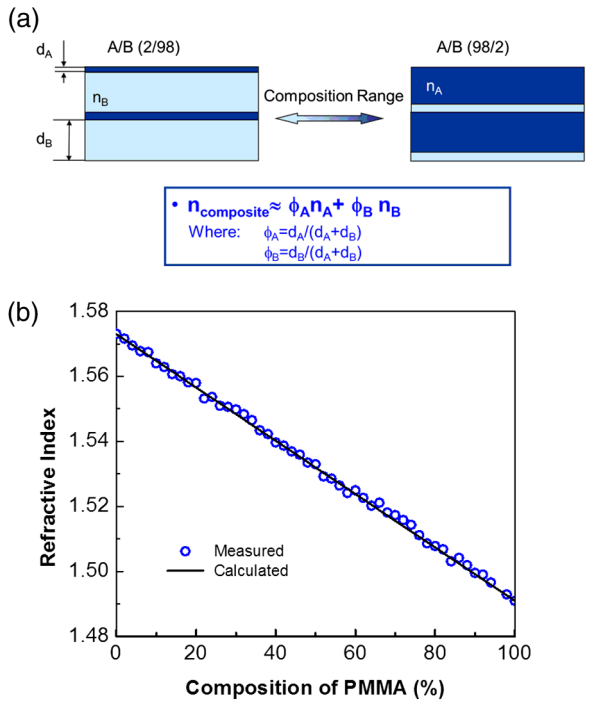

Fig. 2 (a) Films with tailored refractive index and (b) refractive indices of PMMA/SAN17 films.

molding in a concave–convex mold pair. Spherical refractive index contours are created by maintaining the thickness of the curved GRIN preform equal to the difference in the convex and concave mold radii of curvature, as described previously in detail.[22] Curved GRIN preforms can be further transformed into a variety of finished optics by additional diamond turning.

Using this methodology, a variety of GRIN containing geometric lens shapes could be formed that include meniscus lenses, plano-convex, plano-concave, or plano optics. Basically, any machinable, spherical, or aspheric shaped geometric optic can be fabricated with an internal GRIN distribution. Internal GRIN distribution shapes, or internal refractive index curvature, can also be varied between axial, spherical, or a special radial GRIN distribution case in a planar optic similar to a Wood lens.[20] Due to the formability of polymer materials, GRIN optics can be fabricated with a large range of geometric radii and diameters. These radii could be as sharp as 3 mm and approach a nearly planar, infinite radius. GRIN optics with diameters ranging from 6 to 60 mm have been fabricated. As compared to conventional GRIN sol–gel, deposition, or interdiffusion techniques, this nanolayering approach provides many fabrication freedoms enabling breadth, not only in the shape of the optic's refractive index distribution (axial, radial, or aspheric), but also in the optical diameter, optic thickness, and surface curvatures. None of these freedoms significantly change the optical fabrication process. Therefore, grounded in providing optical designs an additional degree of freedom, nanolayered GRIN optical systems offer a materials and fabrication path toward demonstrating previously unattainable optical designs. Indeed, these methods have produced GRIN optics that out-performed similarly powered homogenous optical lens systems.

3 Review of Demonstrator Lens Design

3.1 *Aspheric Human Eye Lens*

The human eye, constructed from a two-element cornea and GRIN lens, Fig. 4, represents one of the most widely studied naturally occurring GRIN optical systems. The human eye produces a nearly aberration-free image.[30] The high performance of the two lens optical system is due to the GRIN lens dual compensator optics which derives corrective power from an aspheric surface geometry and an internal GRIN distribution. Together these correct for corneal induced–spherical aberrations while avoiding off-axis coma.[30] This corrective power originates from the nearly 22,000 nonplanar protein layers that constitute an approximately parabolic shaped optic refractive index gradient. The GRIN decreases from a value of 1.42 at the lens center to $n = 1.37$ at its surface.[11,31] The ability of the human eye lens protein layers to vary its refractive index results from a dynamic chemical make-up, i.e., volumetric ratio of protein to water concentration proportional to the material refractive index, within the layers.

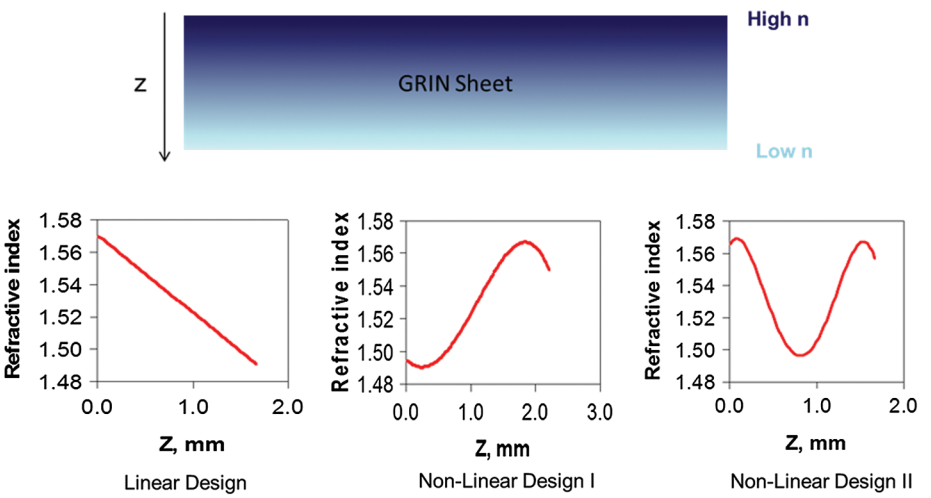

Fig. 3 A schematic showing the flexibility of the nanolayered GRIN technique of making sheets with different refractive index distributions: linear and/or nonlinear.

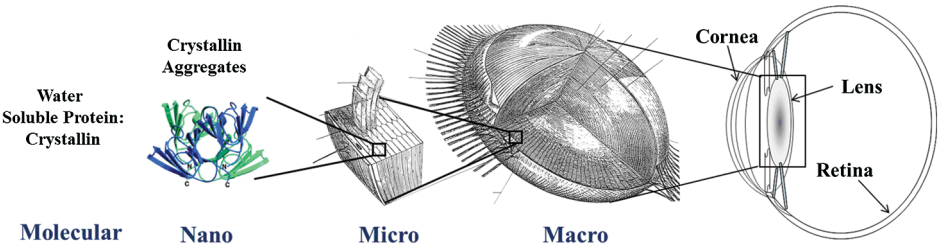

Fig. 4 Hierarchical layered structure of the human eye lens.

Although the shape and GRIN distribution of the human eye lens has been extensively studied,[12,32,33] traditional interdiffusion[19] and sol–gel GRIN fabrication techniques[15,16] have not produced equivalent refractive index distributions. However, the design freedom from combining polymer nanolayered films with thermoforming offers a materials and fabrication pathway capable of producing a bio-inspired synthetic GRIN human eye lens. A summary of the recently published bio-inspired human GRIN eye lens is included to demonstrate that the nanolayered film GRIN optic fabrication technique has the ability to build a lens with any arbitrary refractive index distribution and lens shape.[25]

An optical design based on the geometry and internal refractive index distribution of the human eye lens was selected based on previously published works. One caveat to design a synthetic version of the human eye lens is an age-dependent GRIN distribution and lens geometry.[12,32,33] Based on one such age-dependent human lens model for the refractive index distribution and geometry developed by Diaz et al.,[25] an "Age = 5" human eye lens was selected as a design case. The "Age = 5" model eye possesses a maximum GRIN magnitude in the lens, estimated at $\Delta n = 0.05$, which illustrates the maximum corrective contribution of the GRIN to the lens performance.

The fabrication pathway for the construction of the inspired copy of the human eye lens required fabrication of two aspheric, plano-convex lenses. Both the anterior and posterior lens followed Diaz's model for the refractive index distribution and were translated into a Code V spherical ray tracing model for improved computational and fabrication efficiency, as shown in Fig. 5. A refractive index shift by +0.12 was required in the synthetic eye due to the available polymer material refractive index as compared to the water-biological protein layers of the human eye. This shift in the refractive index value, not in the shape, was accounted for in the design simulations. A final lens design change to the aspheric coefficients of both the anterior and posterior lens of 0.5 and −5.0 were made. This change allowed for the final optic performance to be measurable in an $n = 1.0$ (air) versus an $n = 1.33$ (water) environment [Table 2 and Fig. 5(c)].

The construction of the nanolayered polymer bio-inspired human eye lens was accomplished following the previously described procedure utilizing PMMA/SAN17 nanolayered

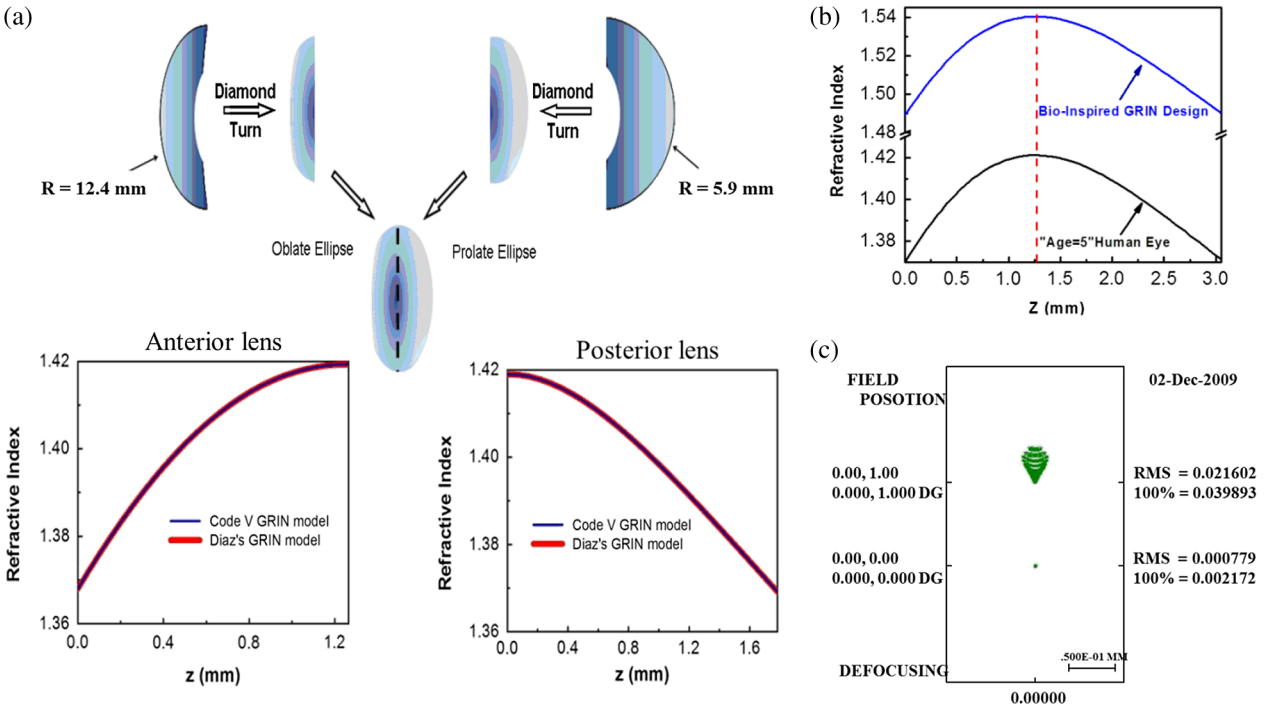

Fig. 5 (a) Process schematic for producing anterior and posterior bio-inspired GRIN lenses. Refractive index distribution of the "Age = 5" human eye lens (anterior and posterior) represented in the Diaz's and Code V models; (b) refractive index plot of the designed bio-inspired GRIN lens in comparison to the Age = 5 lens; and (c) RMS wave error of bio-inspired GRIN lenses with two different aspheric coefficients simulated by Zemax software: (top point) $Q_{\text{anterior}} = -5$ and $Q_{\text{posterior}} = -4$; (bottom point) $Q_{\text{anterior}} = 0.5$ and $Q_{\text{posterior}} = -5$.

Table 2 Geometric parameters of "Age = 5" and bioinspired human eye lenses.

Lens	Thickness (mm)	$R_{anterior}$ (mm)	$Q_{anterior}$	$R_{posterior}$ (mm)	$Q_{posterior}$	Diameter (mm)
Age = 5	3.048	12.4	−5	−5.90	−4	6
Bioinspired	3.048	12.4	0.5	−5.90	−5.0	6

films. The films were stacked, consolidated, shaped, and diamond turned into anterior and posterior GRIN lens according to geometry and GRIN distribution shown in Fig. 5. Nanolayered anterior and posterior refractive index distributions were confirmed through attenuated total reflectance Fourier transform infrared spectroscopy (ATR-FTIR).[25] Diamond turned aspheric anterior and posterior lens surface curvatures were mapped and compared to the prescribed surface profiles by noncontact profilometry with a placido-cone topographer (Fig. 6). Confirmation of the nanolayered polymer GRIN lens geometric and internal refractive index distribution allowed for optical measurements to demonstrate the effect GRIN has on the optical lens performance as compared to an identically shaped homogenous PMMA lens.

The optical performance of the synthetic GRIN optics was measured and compared against a simulated transmission wavefront at the Naval Research Laboratory (Fig. 7). Wavefront measurements of the posterior GRIN and PMMA control lenses were tested with light incident on the planar lens surfaces, i.e., from the same direction as their design.[25] In the lens design, there was no tilt contribution to the wavefront measurement; however, the finished lens possessed a tilt contribution that indicated a level of parallelism achieved in the diamond turning process. The tilt contribution of the wavefront for the posterior GRIN and PMMA control lenses was determined to be 7.6 and 18.8 waves (peak-to-valley), respectively, across the measured aperture [Fig. 7(a) and 7(c)]. These measured results had a good agreement with the numerical simulations [Fig. 7(b) and 7(d)]. The RMS wavefront was reduced from 0.41 in the PMMA reference lens down to 0.2 in the GRIN lens [Fig. 7(b) and 7(d)]. Since the posterior PMMA control and GRIN lenses have the same physical dimensions, the incorporation of a GRIN distribution effectively exhibited less wavefront error in a polymer lens of an identical geometry. It is noted that by holding the optic geometry constant, the PMMA wavefront did not represent an optimized minimum value. However, the change, via a wavefront reduction in this example, in the optics wavefront distortion can be solely attributed to the introduction of a bio-inspired intra-lens refractive index distribution.

Both anterior and posterior GRIN lenses were reversibly assembled into a biconvex human eye GRIN lens with an optical gel. The assembled lens imaged a print logo placed about 33 cm from the bare camera (Fig. 8). Illuminated by an external light source, the camera imaged the logo through the nanolayered bio-inspired "Age = 5" human eye GRIN lens. The resulting image was clear and sharp, confirming the focusing ability of the bio-inspired human eye lens.

The added optical design flexibility provided by the novel nanolayered fabrication process demonstrated in the "Age = 5" bio-inspired, aspheric human eye GRIN lens provides optical engineers an additional design variable, GRIN distribution, to optimize optical systems for enhanced properties. This technology has demonstrated the feasibility of making spherical and aspheric lenses with a nonlinear and nonsymmetrical GRIN distribution. This technique may also enable future potentially implantable, intraocular (IOL) polymer GRIN lenses to replace the deteriorated or destroyed human eye lens. As a material for IOLs, PMMA, a component of the described aspheric human eye lens, has a long history of use as a result of its high light transmission, hydrophobic surface, and ease to add a UV absorber to the monomer with the earliest implantable PMMA IOL tracked back

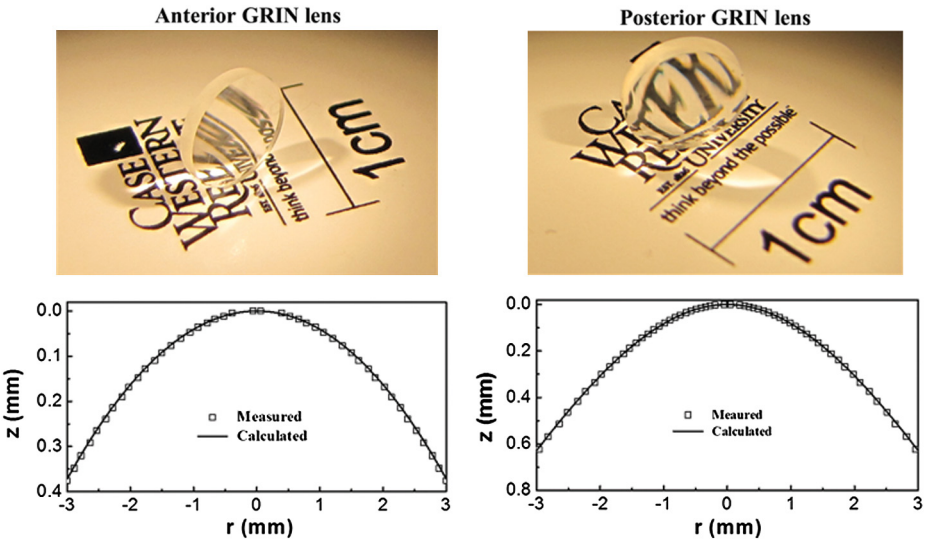

Fig. 6 Images of bio-inspired GRIN lenses (top) and the corresponding cross-sectional profiles of anterior and posterior GRIN lenses (bottom).

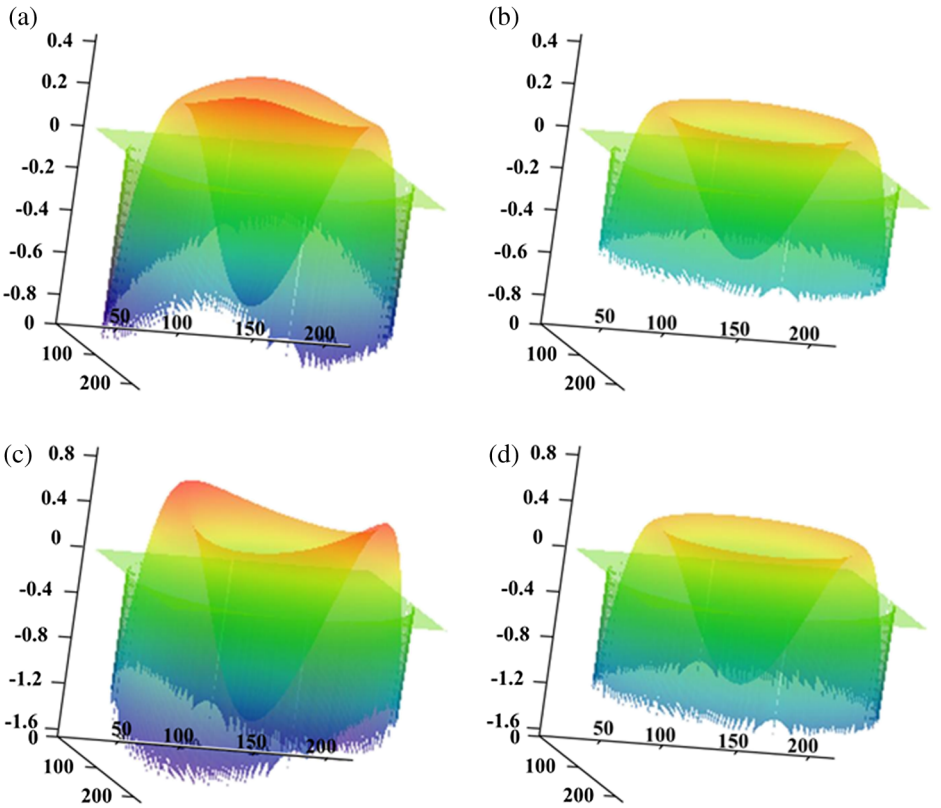

Fig. 7 Plots of experimentally measured and simulated wavefronts for as built bio-inspired aspheric posterior lenses: (a) measured data of GRIN lens; (b) numerically simulated values of GRIN lens; (c) measured data of PMMA reference lens; (d) numerically simulated data of PMMA reference lens. Vertical axis in units of waves (633 nm). Planar values are unit less measures of aperture across the wavefront sensor.

to 1950s.[34,35] Although PMMA IOLs are still used in some countries, usage is waning due to its lack of mechanical flexibility in comparison to deformable IOLs now available. Adoption of a nanolayered GRIN IOL is challenged with introducing material flexibility, as well as an understood deformable optical performance, for medical community adoption of the technology.

3.2 *Spherical GRIN Lens for Size and Weight Reduction*

The flexibility of the polymeric nanolayering approach to GRIN lens fabrication allows for additional design freedom to improve performance over a similar f/# conventional homogenous plastic or glass optics. To demonstrate this advantage, a plano-convex nanolayered GRIN singlet was designed, fabricated, and characterized against a commercial glass optic while simultaneously reducing the optic size and weight. A plano-convex nanolayered GRIN lens was designed by the Naval Research Laboratory to minimize spherical aberration using custom designed ray-tracing software incorporated into ZEMAX (Zemax Development Corporation, Bellevue, WA). Constructed from the previously described family of PMMA and SAN17 nanolayered films, a lens with a spherical refractive index distribution ranging from 1.53 to 1.57 (Fig. 9) was fabricated by stacking and consolidating 128 individual nanolayered films. The films were molded into a meniscus preform, a requirement to establish a spherical refractive index distribution, and diamond turned into a plano-convex singlet as described in Table 3.

The optical properties of the nanolayered GRIN lens were compared against a commercial bi-convex BK7 (Newport Optics Inc., Irvine, CA, part # KBX049) glass lens. The bi-convex BK7 glass lens was chosen to exhibit a similar f/# 2.2 to the f/# 2.4 plano-convex GRIN singlet when the optics were apertured down to 18 mm. That a bi-convex BK7 lens was required to match the f/# of the nanolayered plano-convex lens was a result of the added optical power of the GRIN distribution in the bulk material portion of the lens singlet. In addition to GRIN eliminating one of the glass lens convex surfaces to achieve the target f/#, the lens weighed significantly less, approximately one quarter of that of glass optic, even after normalizing the lenses for an identical optical aperture and removing weight contributions of lens material edge thickness. The large weight reduction resulted from the lower PMMA/SAN17 material density (1.12 g/cm^3) compared to BK7 (2.5 g/cm^3) and the reduction in lens center thickness in the polymer GRIN lens. It is worth noting that the significant weight reduction demonstrated in the 20 mm aperture optics of this study represents a GRIN advantage that will only widen as the comparative optic diameter and thickness increase in larger optic designs.

Simplifying the optic's geometry and reducing its weight can be realized only if the GRIN optic can exhibit performance similar to a homogenous lens. To characterize and compare the optical performance, spot size and contrast measurements were completed on both optics. Monochromatic spot sizes of the GRIN and BK7 lens were characterized

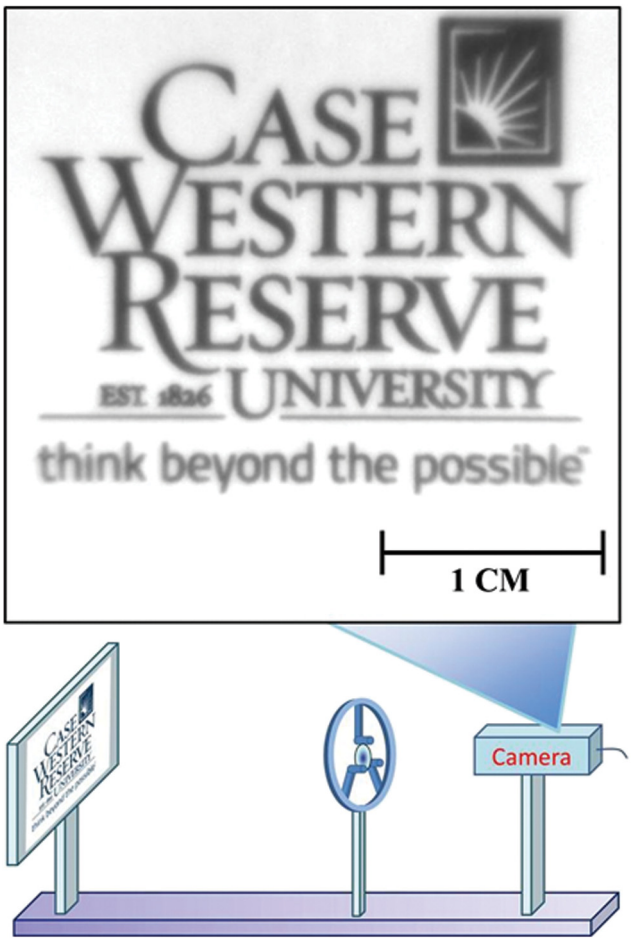

Fig. 8 A Case Western Reserve University logo image that was focused using a bio-inspired "Age = 5" human eye GRIN lens and captured with a CCD camera.

by focusing a collimated HeNe laser beam with a wavelength of 632.8 nm and measuring maximum transmission through a 50 μm pin hole at the lens focus point [Fig. 10(a)]. Next, a 1-D intensity scan of the focused HeNe spot size was measured for both lenses [Fig. 11(c)]. The polymer GRIN lens exhibited a sharper decrease in spot size intensity and a higher image contrast. One-dimensional intensity scan of these spots was accomplished by measuring the full width at half-maximum peak height of the GRIN and BK7 lens.

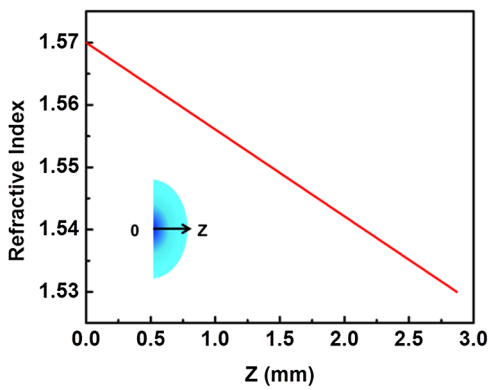

Fig. 9 Refractive index distribution of the PMMA/SAN17 polymer GRIN lens (in the *Z* direction).

Table 3 Design specification for the f/2.25 GRIN lens.

Lens diameter	20 mm
Clear aperture	18 mm
Form factor	Plano-convex
Radius of curvature	23.5 mm
Center thickness	2.87 mm
Focal length	41.2 mm
f/#	2.25
Minimum index	1.53
Maximum index	1.57

The half-maximum peak heights were measured at 100 and 200 μm for the polymer GRIN and BK7 lenses, respectively. As expected, with a tighter focal spot, the comparison of a USAF test chart image of the nanolayered polymer GRIN lens displayed a greater contrast and higher intensity than that of the BK7 lens (Fig. 11). The USAF air force patterns were imaged through the polymeric GRIN and BK7 glass at 630 nm using an identical CCD camera and lens to image spacing.[23]

The combined superior optical performance and weight savings of the nanolayered GRIN lens over a commercial BK7 optic demonstrate the technology potential to improve lens performance through the reduction of spherical aberration, while simultaneously reducing the size of conventional imaging systems. Additional optical modeling and fabrication studies have demonstrated the extension of this lens singlet performance in an optical system. Incorporation of two nanolayered GRIN optics in a five lens night vision imaging system was designed and characterized to exhibit similar optical performance while encompassing only 1/7 the weight of the homogenous optic system. The corrective power of the nanolayered GRIN technology is not limited solely to monochromatic spherical aberration corrections and has been demonstrated to also affect chromatic aberrations.

Traditional achromatic optic elements are doublets comprising highly dispersive flint glass and lower dispersion crown glass arranged with geometric surface curvatures selected to balance material chromatic affects. Optical design simulations have recently demonstrated the ability of a model nanolayered polymer material system to achieve a red-blue achromat singlet utilizing spherical and/or aspheric surfaces.[26] Chromatic correction of the nanolayered optics was achieved by decoupling the internal spherical GRIN contours with the surface curvature of the optics. The highest powered achromat lenses were demonstrated when the GRIN contours were created in the opposite direction to the lens surface curvature, i.e., bulk polymer layers possessing a convex internal refractive index contour in an optic with a geometric concave surface profile. A specific design case was presented that demonstrated a 0.1-μm focal shift over 470

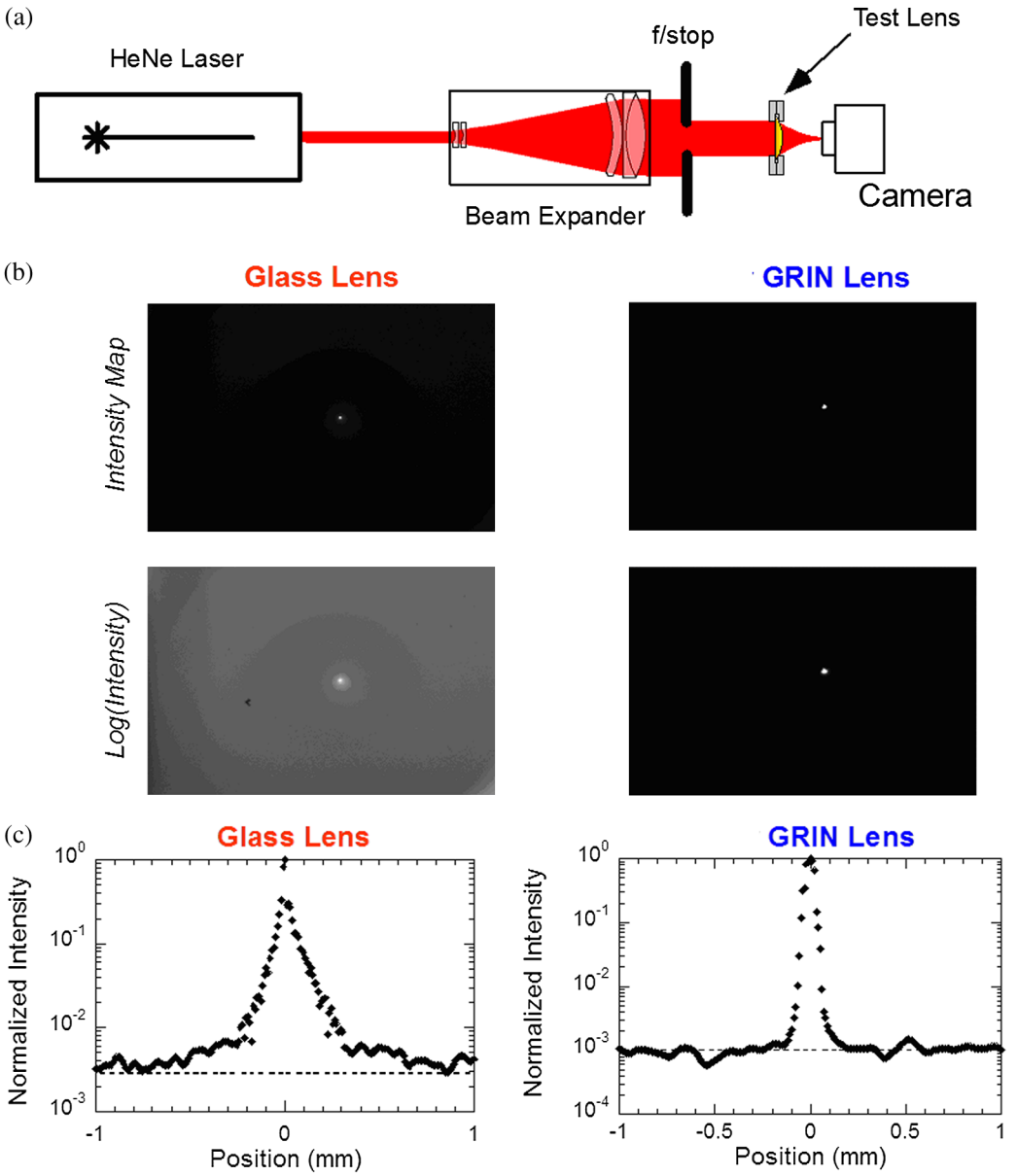

Fig. 10 (a) Experimental setup of minimum spot size measurement; (b) spot size of glass lens and PMMA/SAN17 polymer GRIN lens; and (c) 1-D intensity plot of focal spot image.

to 660 nm operating band for a 19-mm diameter nanolayered plano-convex achromat singlet optic.

Though a significant achievement, the simulated ability of the nanolayered GRIN technology to produce achromatic singlet elements is not without challenges. Materials utilized in the previously referenced effort utilized "typical polymer" optical properties in designing the achromatic singlet. The universe of existing nanolayered polymer material systems needs to be expanded to account for a high refractive index ($n \sim 1.70$) and highly disperse (abbe number ~ 20) material candidate. It should be stated that polyester-type polymer materials with similar optical properties exist; however, optics utilizing the polymer nanolayering process for the production of achromatic optics is still under development. An additional polymer material pair containing a fluoropolymer and acrylic material is under development to expand the available nanolayered material Δn to encompass values from 1.40 to 1.57. The addition of this new material system will address some of the optical corrective challenges encompassed with designing a polychromatic corrected element with the same degrees of freedom as utilized in the previous monochromatic aberration corrected example. An opportunity to combine the new optical polymer materials with GRIN correction for chromatic aberration with unconventional, or even aspheric, geometries would yield a singlet optic simultaneously corrected for spherical and chromatic aberrations. An original research effort toward a nontraditional, GRIN ball lens is described in the next section as a potential path toward future efforts to explore potential GRIN optical advantages.

3.3 *New GRIN Development: Layered GRIN Ball Lens*

Spherical or ball lenses have been a source of optical designs for hundreds of years. Full sphere lenses are attractive due to

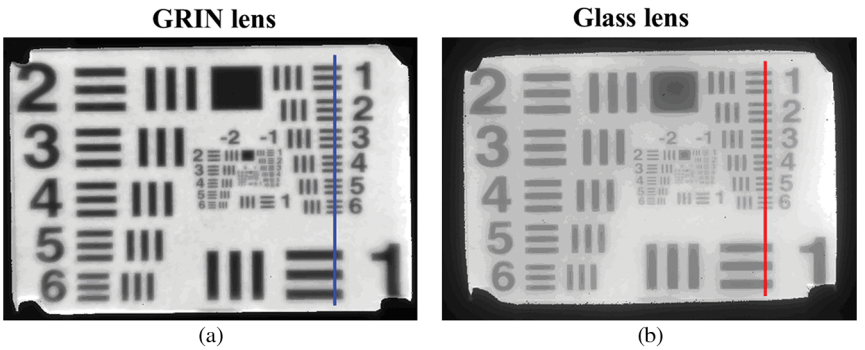

Fig. 11 USAF test chart imaged through a PMMA/SAN17 polymer GRIN lens (a) and a glass lens (b).

their low f/# and potential for wide field of views. Optical ball lens designs from Maxwell and Rudolf Luneburg proposed incorporating large GRIN distributions with a core refractive index of 2.0 reducing radially to 1.0 refractive index at its lens surface, to reduce or eliminate aberrations.[24,36] Although some ball lenses are applied in microwave technology,[37,38] many GRIN ball lens solutions have remained elusive in optics systems due to the GRIN material or fabrication limitations. Limitations of the current GRIN technologies arise from the depth of gradient, magnitude of GRIN change (Δn), and refractive index distribution control. The design flexibility of the novel nanolayered

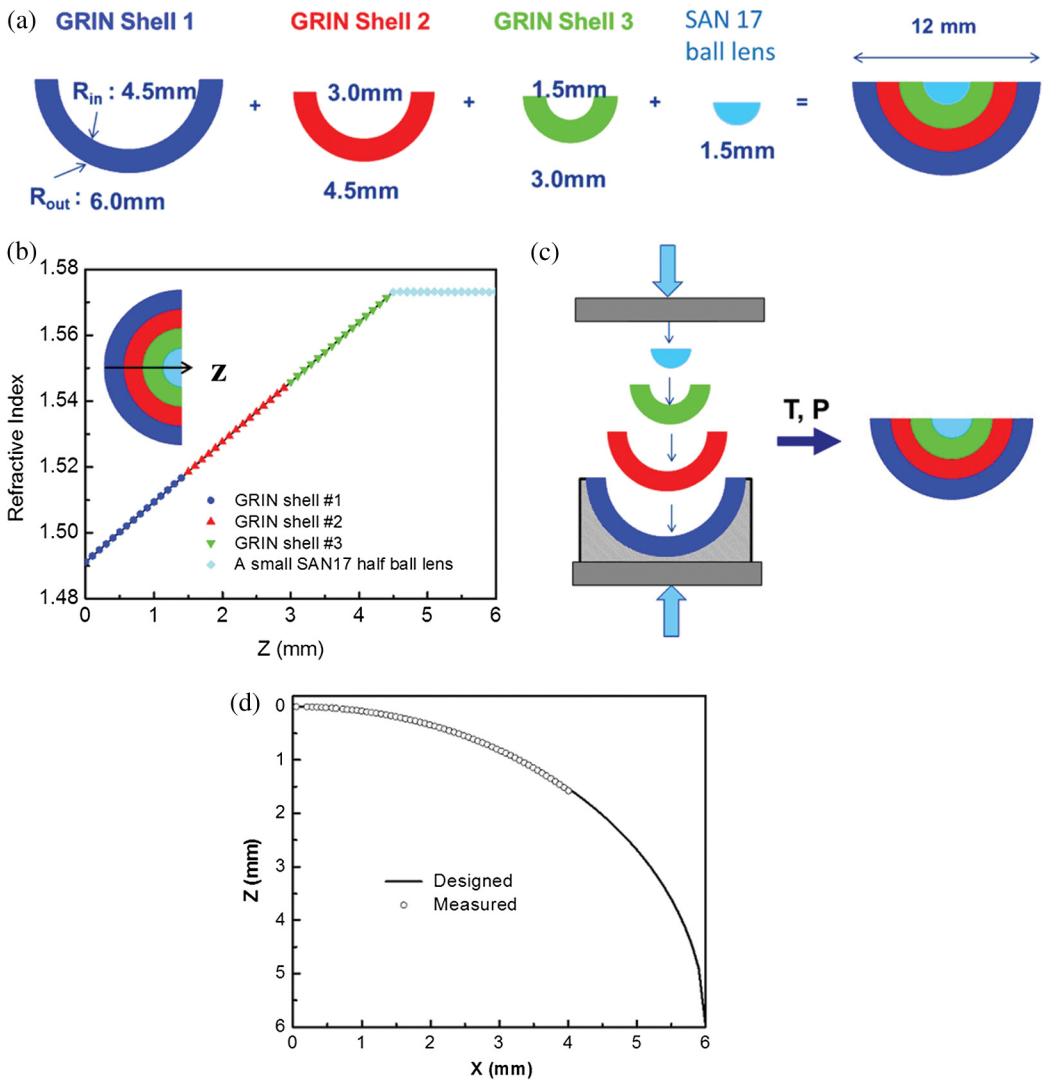

Fig. 12 (a) Schematic representation of a hemispherical GRIN lens; (b) refractive index distribution design of a hemispherical GRIN lens in the *Z* direction; (c) procedure of thermoforming a hemispherical GRIN lens; and (d) cross-sectional profile of the hemispherical GRIN lens acquired with placido-cone topography.

polymer GRIN technology was utilized to demonstrate a basic capability to fabricate GRIN ball lens with arbitrary refractive index profiles up to a 12-mm diameter.

A path to fabricating a ball GRIN lens was derived through a creation of a series of spherical nesting shells which could be adhered together into the ball optic. As illustrated in Fig. 12, a small SAN17 half ball was adhered inside three nesting GRIN shells of different geometric radii, labeled GRIN shell 1, GRIN shell 2, and GRIN shell 3. The three nesting GRIN shells were fabricated with the full available refractive index range of the nanolayered optical PMMA/SAN17 films, which spanned 1.49 to 1.57. This refractive index distribution, Δn of 0.08, was divided equally throughout the three shells. The three nesting GRIN shells and half ball were compressed into a hemispherical GRIN lens with a diameter of 12 mm, as illustrated in Fig. 12(c). The cross-section profile of the hemispherical GRIN lens near the vertex was characterized confirming the desired geometric design radius via noncontract profilometry with a placido-cone topography, as shown in Fig. 12(d). Measurements far from the ball lens vertex were not measurable due to the limited field of view and depth-of-focus of the placido-cone topography.

Radial half-ball focal lengths of the GRIN lens (Fig. 13) were compared against a hemispherical homogenous PMMA control lens and simulated performance of a homogenous SAN17 lens. A hemispherical geometry lens was utilized for focal length measurements to ensure that the optic focal length was outside the lens surface enabling the characterization through conventional optical metrology techniques. As expected, the change in focal length as a function of optical aperture of the half-ball GRIN lens was significantly less than an identically shaped homogenous PMMA (measured) or a simulated SAN17 lens result in the following equation

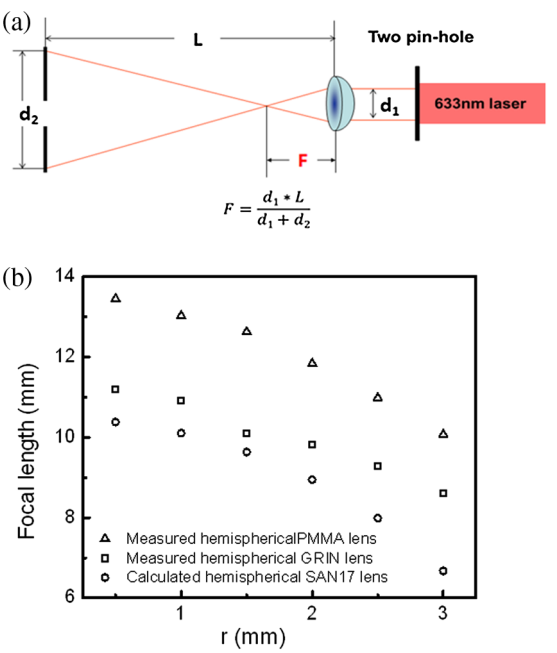

Fig. 13 (a) Experimental setup for focal length measurements; and (b) focal length for PMMA control and hemispherical GRIN lenses as a function of distance between two pinholes: hemispherical GRIN lens (triangle) and PMMA control lens (square).

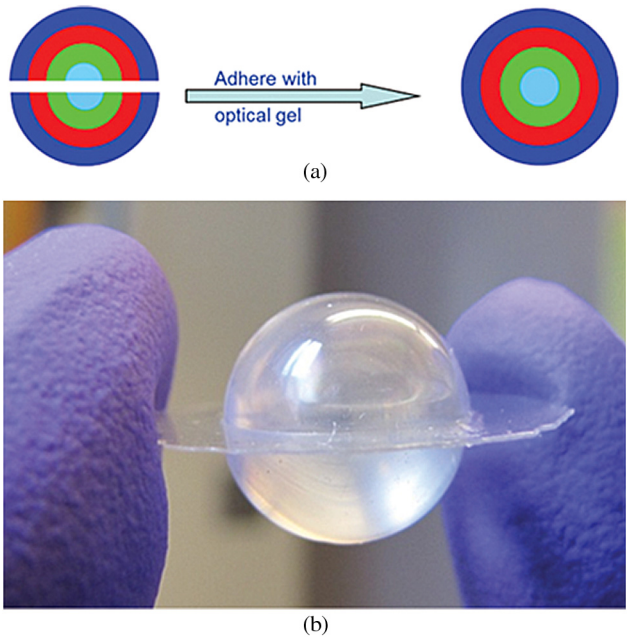

Fig. 14 Method of adhering two hemispherical GRIN lenses (a) and image of a GRIN ball lens (b).

$$\frac{1}{F} = \left((\sqrt{R^2 - r^2}) + \frac{r}{\tan\left[\arcsin\left(\frac{r \times n_{\text{lens}}}{R \times n_{\text{air}}}\right) - \arcsin\left(\frac{r}{R}\right)\right]} - R \right)^{-1}, \quad (1)$$

where R is the radius of the SAN17 hemispherical lens; r is the distance from the optical axis; n_{lens} is refractive index of the SAN17 hemispherical lens; and n_{air} is the refractive index of air. This result confirmed the added power of the GRIN to correct for spherical aberration in a hemispherical optic construction as the radially dependent optic focal length ($\Delta FL/\Delta r$) value of GRIN lens is much smaller than those of both PMMA and SAN17 homogenous lenses. A final step to create a full spherical GRIN ball lens was accomplished by adhering to the two hemispherical GRIN lenses as shown in Fig. 14.

The nanolayering polymer materials system was utilized to demonstrate a production path toward the fabrication of spherical GRIN ball lenses with up to a $\Delta n = 0.08$. Beyond this accomplishment, the nanolayering fabrication technology allows for almost any shape refractive index distribution to be created in future designs. Potential applications for the incorporation of a novel GRIN ball lens include the wide field-of-view solar concentrators and compact imaging systems such as UAV cameras, surveillance, and panoramic imaging systems.

4 Conclusion and Projected Future Impacts

Inspired by the structure of biological optic systems, the nanolayered polymer film approach to designing and fabricating GRIN lenses with arbitrary refractive index distribution profiles along with independently prescribed lens surface geometries has enabled the design and fabrication of a whole new class of gradient index optics. Nanolayered polymer coextrusion processing has been demonstrated to produce an inventory of materials with a tailored

refractive index that were utilized to construct a discretely stepped GRIN distribution. Thermoforming of these GRIN materials was utilized to create axial or spherical distributions in spherical, aspheric, or planar optics. Topography, spectroscopy, and optical wave front or contrast imaging confirmed the ability of the nanolayered polymer GRIN lens fabrication process to create optics with the desired shape, internal refractive index distribution, and optical performance.

First-generation nanolayered polymer GRIN lens designs and optics were fabricated to demonstrate the unique ability to construct optics previously rendered un-buildable due to a combination of materials and/or fabrication restrictions which include: optic size, lens surface curvature, and/or magnitude and curvature of the internal GRIN profile. A polymeric, nanolayered aspheric GRIN optic was fabricated which mimicked the refractive index distribution and layered construction of a human eye lens. This optic demonstrated an improved performance with the inclusion of the GRIN over a homogenous PMMA aspheric lens with an identical optic geometry. A plano-convex nanolayered polymer GRIN lens was designed, fabricated, and demonstrated to show an optical performance advantage over a similar f/# homogenous BK7 bi-convex lens while also significantly reducing the optic weight. Finally, a new class of GRIN ball lenses was fabricated as proof-of-concept to show a path toward the production of classically studied, but never built Maxwell or Luneburg-like spherical GRIN lenses. The ability to create ball lenses with an arbitrary spherical refractive index distribution represents a potential to realize optics with a wide field of view and minimal geometric-induced aberrations. The nanolayered fabrication approach to the GRIN ball lenses will also allow scalability of lens diameters from small, 6 mm, to large, approaching an inch or more, enabling potential applications in handheld or equipment mounted surveillance or light concentrating applications.

We believe that the demonstrator nanolayered GRIN optics fabricated to-date captures the spirit of the advantages afforded by the highly flexible fabrication process, however, encompasses only a sampling of the potential application space for this technology. All the described optics in this paper were built utilizing a PMMA/SAN17 material system, whereas the nanolayering technology is not restricted to these materials. The vast array of available polymer materials provides an opportunity for research and development of additional polymer material systems with contrasting or complementary refractive index ranges, dispersion properties, operating temperature, and physical properties for GRIN optic construction. On-going research at CWRU hopes to exploit the nature of polymer materials to potentially expand the nanolayered GRIN technology into areas of elastically deformable polymers which may even produce variable focal length optics as a function of an external pressure or electronic/chemical stimulus.

Acknowledgments

The authors would like to acknowledge instrumental ideation and development support from Dr. James Shirk, Dr. Guy Beadie and his Naval Research colleagues, and Dr. Narkis Shatz. This research was generously supported by the Defense Advanced Research Projects Agency (Contract HR0011-10-C-0110) and the NSF Center of Layered Polymeric Systems (Grant DMR-0423914).

References

1. B. K. Pierscionek and J. W. Regini, "The gradient index lens of the eye: an opto-biological synchrony," *Prog. Retinal Eye Res.* **31**(4), 332–349 (2012).
2. D. E. Nilsson, "Vision optics and evolution: nature's engineering has produced astonishing diversity in eye design," *Bioscience* **39**(5), 298–307 (1989).
3. M. F. Land and R. D. Fernald, "The evolution of eyes," *Ann. Rev. Neurosci.* **15**(1), 1–29 (1992).
4. W. S. Jagger and P. J. Sands, "A wide-angle gradient index optical model of the crystalline lens and eye of the rainbow trout," *Vision Res.* **36**(17), 2623–2639 (1996).
5. W. S. Jagger and P. J. Sands, "A wide-angle gradient index optical model of the crystalline lens and eye of the octopus," *Vision Res.* **39**(17), 2841–2852 (1999).
6. R. H. H. Kroger and A. Gislen, "Compensation for longitudinal chromatic aberration in the eye of the firefly squid, Watasenia scintillans," *Vision Res.* **44**(18), 2129–2134 (2004).
7. D. E. Nilsson et al., "Advanced optics in a jellyfish eye," *Nature* **435**(7039), 201–205 (2005).
8. M. F. Land, "Optics and vision in invertebrates," in *Handbook of Sensory Physiology*, H. Autrum, ed., Vol. VII/6B, pp. 471–592, Springer-Verlag, Berlin, FRG (1981).
9. B. Pierscionek, "Species variability in optical parameters of the eye lens," *Clin. Exp. Optom.* **76**(1), 22–25 (1993).
10. R. C. Augusteyn and A. Stevens, "Macromolecular structure of the eye lens," *Prog. Polym. Sci.* **23**(3), 375–413 (1998).
11. J. F. Koretz and G. H. Handelman, "How the human eye focuses," *Sci. Am.* **259**(1), 92–99 (1988).
12. J. A. Díaz, C. Pizarro, and J. Arasa, "Single dispersive gradient-index profile for the aging human eye lens," *J. Opt. Soc. Am. A* **25**(1), 250–261 (2008).
13. G. Zuccarello et al., "Materials for bio-inspired optics," *Adv. Mater.* **14**(18), 1261–1264 (2002).
14. D. K. Tagantsev et al., "Phosphate glasses for GRIN structures by ion exchange," *J. Non-Crystal. Solids* **354**(12), 1142–1145 (2008).
15. Y. Koike, Y. Sumi, and Y. Ohtsuka, "Spherical gradient-index sphere lens," *Appl. Opt.* **25**(19), 3356–3363 (1986).
16. Y. Koike, Y. Takezawa, and Y. Ohtsuka, "New interfacial-gel copolymerization technique for steric GRIN polymer optical waveguides and lens arrays," *Appl. Opt.* **27**(3), 486–491 (1988).
17. W. A. Reed, M. F. Yan, and M. J. Schnitzer, "Gradient-index fiber-optic microprobes for minimally invasive in vivo low-coherence interferometry," *Opt. Lett.* **27**(20), 1794–1796 (2002).
18. T. Zentgraf et al., "Plasmonic Luneburg and Eaton lenses," *Nat. Nanotechnol.* **6**(3), 151–155 (2011).
19. D. T. Moore, "Gradient-index optics: a review," *Appl. Opt.* **19**(7), 1035–1038 (1980).
20. E. Baer, P. A. Hiltner, and J. S. Shirk, "Multilayered polymer gradient index (GRIN) lenses," U.S. Patent No. 7,002,754 B2 (Feb. 21, 2006).
21. J. S. Shirk et al., "Biomimetic gradient index (GRIN) lenses," *NRL Rev.*, pp. 53–61 (2006).
22. Y. Jin et al., "New class of bio inspired lenses with a gradient refractive index," *J. Appl. Poly. Sci.* **103**(3), 1834–1841 (2007).
23. G. Beadie et al., "Optical properties of a bio-inspired gradient refractive index polymer lens," *Opt. Express* **16**(15), 11540–11547 (2008).
24. P. Kotsidas, V. Modi, and J. M. Gordon, "Gradient-index lenses for near-field imaging and concentration with realistic materials," *Opt. Express* **19**(16), 15584–15595 (2011).
25. S. Ji et al., "A bio-inspired polymeric gradient refractive index (GRIN) human eye lens," *Opt. Express* **20**(24), 26746–26754 (2012).
26. R. A. Flynn et al., "Achromatic GRIN singlet lens design," *Opt. Express* **21**(4), 4970–4977 (2013).
27. M. Sandrock et al., "A widely tunable refractive index in a nanolayered photonic materials," *Appl. Phys. Lett.* **84**(18), 3621–3623 (2004).
28. T. Kazmierczak et al., "Polymeric one-dimensional photonic crystals by continuous coextrusion," *Macromol. Rapid Commun.* **28**(23), 2210–2216 (2007).
29. M. Ponting, A. Hiltner, and E. Baer, "Polymer nanostructures by forced assembly: process, structure, properties," *Macromol. Symp.* **294**(1), 19–32 (2010).
30. P. Artal and J. Tabernero, "The eye's aplanatic answer," *Nat. Photon.* **2**(10), 586–589 (2008).
31. R. D. Fernald and S. E. Wright, "Maintenance of optical quality during the lens growth," *Nature* **301**, 618–620 (1983).
32. M. Dubbeleman, G. L. Van der Heijde, and H. A. Weber, "Change in shape of the aging human crystalline lens with accommodation," *Vision Res.* **45**(1), 117–132 (2005).
33. C. E. Campbell, "Nested shell optical model of the lens of the human eye," *J. Opt. Soc. Am. A* **27**(11), 2432–2441 (2010).

34. D. J. Apple et al., "Complications of Intraocular Lenses. A Historical and Histopathological Review," *Surv. Ophthalmol.* **29**(1), 1–54 (1984).
35. J. L. Guell et al., "Phakic intraocular lenses part 1: historical overview, current models, selection criteria, and surgical techniques," *J. Cataract Refract. Surg.* **36**(11), 1976–1993 (2010).
36. A. D. Falco, S. C. Kehr, and U. Leonhardt, "Luneburg lens in silicon photonics," *Opt. Express* **19**(6), 5156–5162 (2011).
37. H. F. Ma and T. J. Cui, "Three-dimensional broadband and broad-angle transformation-optics lens," *Nat. Commun.* **1**, 124–130 (2010).
38. N. Kundtz and D. R. Smith, "Extreme-angle broadband metamaterial lens," *Nat. Mater.* **9**(12), 129–132 (2009).

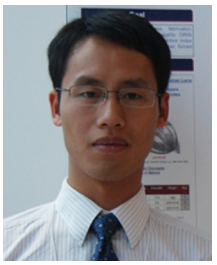

Shanzuo Ji received a BEng degree in material science and engineering from Southwest Jiaotong University, China, in 2006 and MS degree in polymer chemistry and physics from Zhejiang University, China in 2008. He is currently a PhD candidate studying polymer science and engineering at Case Western Reserve University. His research interests include structure-property relationships of polymers, multilayered polymeric systems, gradient refractive index (GRIN) materials and lenses, shape memory polymers, and gas sensitive materials.

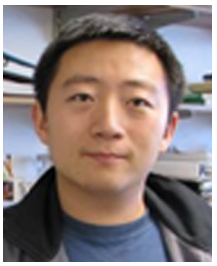

Kezhen Yin earned a BS degree in polymer science and engineering from Zhejiang University, China, in 2008 and MS in material science and engineering from South Dakota School of Mines & Technology. He is currently a PhD candidate in macromolecular science and engineering at Case Western Reserve University with a research focus on nanolayered bio-inspired polymer GRIN lens and polymer dielectric films.

Matthew Mackey attended Lafayette College where he graduated Magna Cum Laude with a BS degree in chemical engineering. He then went on to graduate school at Case Western Reserve University where his research focus was on polymer dielectrics for high-energy density capacitor applications. Matthew received his PhD in chemical engineering at Case Western Reserve University in 2012. He expanded his research interests to include polymer micro and nano fibers, polymer optics, and capacitor prototyping as a research associate at CWRU.

Aaron Brister graduated from Case Western Reserve University in 2007 with a MS degree in physiology and biophysics. He spent several years working in a rapidly expanding biotechnology start-up as a research scientist and project manager. Here, while focusing on applied research and engineering, he collaborated with scientists, engineers, economists, and businessmen, learning skills from each and an interdisciplinary, team-science work approach. Since then, he returned to Case, taking a more academic position. Now he works for the National Science Foundation Science and Technology Center at its Case headquarters, expanding his team-science skills, as a project manager for its development work and grant writing activities while also teaching.

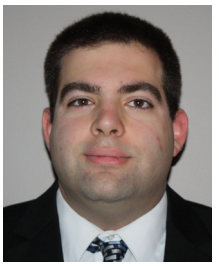

Michael Ponting is a co-founder and President of PolymerPlus LLC where he serves as the lead scientist and primary investigator on several multilayered-based technology development contracts. A 2010 PhD graduate of the Case Western Reserve University Department of Chemical Engineering under Professors Eric Baer and Anne Hiltner, he has more than 20 peer-reviewed publications, conference papers, and pending patent applications related to the production and structure property relationships of multilayered polymer film systems. His research interests include, processing of micro- and nanolayered polymer systems, multilayer die design, polymer structure-property relationships, polymer optical properties, and manufacturing/metrology of nanolayered polymer gradient index optics.

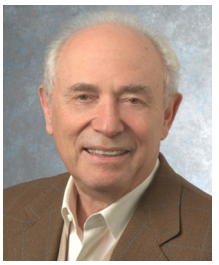

Eric Baer is director of the center for Layered Polymeric Systems (CLiPS) and is the Herbert Henry Dow professor of science and engineering and professor of macromolecular science and engineering at Case Western Reserve University. Honors include the Curtis W. McGraw Research Award, American Society of Engineering Education, 1968; International Award of the Society of Plastics Engineers, 1980; Borden Award in the Chemistry of Plastics and Coatings, International Education Award of the Society of Plastics Engineers, 1991; Doctor of Sciences "honoris causa" of the Russian Academy of Sciences (Chemistry), 1993; Paul J. Flory Education Award, American Chemical Society, 1996; inducted into The Plastics Hall of Fame, 2000; Honored as distinguished university professor of Case Western Reserve University, 2011. His research interests include, irreversible microdeformation mechanisms relationships between hierarchical structure and mechanical function; polymer composites and blends; and micro- and nanolayered composites. He is the editor of five books and over 600 publications.